PHYSICAL REVIEW D 79, 045020 (2009)

Dark matter in the MSSM golden region

Junya Kasahara,[1,*] Katherine Freese,[2,†] and Paolo Gondolo[1,‡]

[1]*Department of Physics, University of Utah, 115 South 1400 East, Suite 201, Salt Lake City, Utah 84112-0830, USA*
[2]*Michigan Center for Theoretical Physics, Physics Department, University of Michigan, Ann Arbor, Michigan 48109, USA*
(Received 5 June 2008; published 25 February 2009)

Dark matter is examined within the "golden region" of the minimal supersymmetric standard model. This region satisfies experimental constraints, including a lower bound on the Higgs mass of 114 GeV, and minimizes fine-tuning of the Z boson mass. Here we impose additional constraints (particularly due to experimental bounds on $b \to s\gamma$). Then we find the properties of the dark matter in this region. Neutralinos with a relic density that provides the amount of dark matter required by cosmological data are shown to consist of a predominant gaugino (rather than Higgsino) fraction. In addition, the $U(1)_Y$ gaugino mass parameter must satisfy $M_1 \lesssim 300$ GeV.

DOI: 10.1103/PhysRevD.79.045020 PACS numbers: 12.60.Jv, 98.80.Cq

I. INTRODUCTION

The minimal standard supersymmetric model (MSSM) is the simplest supersymmetric extension beyond the standard model of particle physics, and stands to be tested in the upcoming Large Hadron Collider experiments at CERN. The MSSM not only addresses fundamental questions in particle physics, but also naturally provides a compelling dark matter candidate, the lightest supersymmetric particle (LSP). In particular, the neutralino, which is a linear combination of the supersymmetric partners of the photon, the Z boson, and the neutral scalar Higgs particles, has the right cross section and mass to automatically provide the observed density of cold dark matter in the universe. According to the analysis in [1], the latter has the value

$$\Omega_\chi h^2 = 0.1143 \pm 0.0034. \tag{1}$$

Here the subscript χ refers to neutralinos, h is the Hubble constant H_0 in units of 100 km/s/Mpc, and $\Omega_\chi = \rho_\chi/\rho_c$ is the fraction of the neutralino density ρ_χ in units of the critical density $\rho_c = 3H_0^2/(8\pi G) \sim 10^{-29}h^2$ g/cm^3 (alternatively, $\Omega_\chi h^2$ is the neutralino mass density in units of 18.79 yg/m^3).

Perelstein and Spethmann [2] examined a particularly interesting region of MSSM parameter space which they dubbed the "golden region." (A similarly motivated region was previously studied in [3].) Perelstein and Spethmann argued that data and naturalness (i.e. a low degree of fine-tuning) point to a region within the Higgs and top sectors where the experimental bounds from nonobservation of superpartners and the Higgs boson are satisfied and fine-tuning is close to the minimum possible value. They found that, in this region, (i) the two stop eigenstates have masses below 1 TeV, (ii) there is a significant mass splitting between the two stop mass eigenstates, typically $\delta m \gtrsim$ 200 GeV, and (iii) the stop mixing angle must be nonzero. They then suggested collider signatures of the golden region that may be found at the LHC.

In this paper, we further examine this golden region, with a particular focus on discovering the properties of the dark matter within it. We use the numerical package DARKSUSY [4] to find the same golden region as [2], and apply additional constraints due to experimental bounds on $b \to s\gamma$ as well. Then we look for the parameter regime inside the remaining golden region that also gives the right relic density of neutralino dark matter.

Below we begin by reviewing the boundaries of the golden region, and then turn to the properties of the dark matter within it.

II. THE MSSM GOLDEN REGION

We work in the framework of the MSSM. For practical reasons, and to match the choices in [2], we impose the following restrictions on the MSSM parameters at the weak scale. (1) We assume that all soft parameters are flavor diagonal. (2) We assume common soft mass parameters for the first- and second-generation squarks, $m_{\tilde{q}} = m_{Q^{1,2}} = m_{U^{1,2}} = m_{D^{1,2}}$, where m_{Q^α}, m_{U^α}, and m_{D^α} are the soft-supersymmetry breaking masses for the left-handed quark doublets, the up-type right-handed quark singlets, and the down-type right-handed quark singlets, respectively. Similarly, for the sleptons, we assume that all slepton mass parameters are equal, $m_{\tilde{\ell}} = m_{L^{1,2,3}} = m_{E^{1,2,3}}$, where m_{L^i} and m_{E_i} are the singlet and doublet lepton soft mass parameters. (3) We set all tridiagonal soft-supersymmetry breaking terms A to zero except for a large stop trilinear term A_t. (4) We further assume that the third-generation soft mass $m_{D^3} = m_{\tilde{q}}$, but let m_{Q^3} and m_{U^3} vary independently.

We are left with 11 free parameters: the Higgs mass parameter μ; the mass m_A of the CP-odd Higgs boson; the ratio $\tan\beta$ of the Higgs vacuum expectation values; the

*kasahara@physics.utah.edu
†ktfreese@umich.edu
‡paolo@physics.utah.edu

gaugino mass parameters M_1, M_2, M_3; the soft parameters $m_{\tilde{q}}$ and $m_{\tilde{\ell}}$; and the third-generation soft parameters m_{Q^3}, m_{U^3}, and A_t. Furthermore, following [2], we replace the last three parameters (m_{Q^3}, m_{U^3}, and A_t), the mass difference $\delta m = \tilde{m}_2 - \tilde{m}_1$ between the heaviest ($\tilde{m}_2$) and lightest ($\tilde{m}_1$) stop masses, and the stop mixing angle θ_t. Finally, we use $m_t = 174.3$ GeV for the top-quark mass, and define all parameters at the weak scale.

We scan the 11-dimensional parameter space by generating random values of the parameters. The experimentally verified boundaries will be implemented later on for the code run. In scanning parameters, we leave extra margins outside the experimentally allowed domain, so that all experimentally allowed parameters are examined in the scan. Thus, the parameter scan boundaries are wider than the experimentally verified bounds. Here are the parameter scan domains we use (all dimensionful parameters are in GeV):

$$80 < \mu < 500, \qquad 100 < m_A < 2000, \qquad \tan\beta = 10, \tag{2}$$

$$100 < M_1 < 400, \qquad 100 < M_2 < 2000, \qquad 100 < M_3 < 2000, \tag{3}$$

$$100 < m_{\tilde{q}} < 2000, \qquad 100 < m_{\tilde{\ell}} < 2000, \tag{4}$$

$$100 < \tilde{m}_1 < 1000, \qquad 100 < \delta m < 600, \qquad \theta_t = \pi/4. \tag{5}$$

Notice that we fixed the value of θ_t and $\tan\beta$ to reproduce one of the panels in Fig. 2 of [2]. We define our "default scan" to be the case where these values are fixed at $\tan\beta = 10$ and $\theta_t = \pi/4$. We set the fine-tuning level to be 3% (see Sec. II B for details). We also produced other special scans: we randomized $\tan\beta$ in the range 0.5 to 30; we implemented the grand unified theory (GUT) relation between M_1, M_2, and M_3; and we separately extended M_1 up to 2000 GeV.

The points in Fig. 1 illustrate the golden region we obtain in our default scan. This figure can be directly compared with Fig. 2 of [2], from which the solid triangular region is drawn. The dashed-dotted region is obtained using the Perelstein and Spethmann code, but with our value of the top-quark mass. Using DARKSUSY, we have improved upon the previous work by applying more accurate calculations of the Higgs boson mass and of the $b \to s\gamma$ branching ratio, as described below. A variety of other experimental constraints are applied as well, using their implementation in DARKSUSY. In particular, LEP2 searches for direct production of charginos and stops constrain the chargino and stop masses to $m_{\tilde{\chi}^+} \gtrsim 94$ GeV and $\tilde{m}_1 \gtrsim 92$ GeV (these limits are implemented in DARKSUSY). The $b \to s\gamma$ decay rate [5] also constrains the golden region. We use the default range in DARKSUSY,

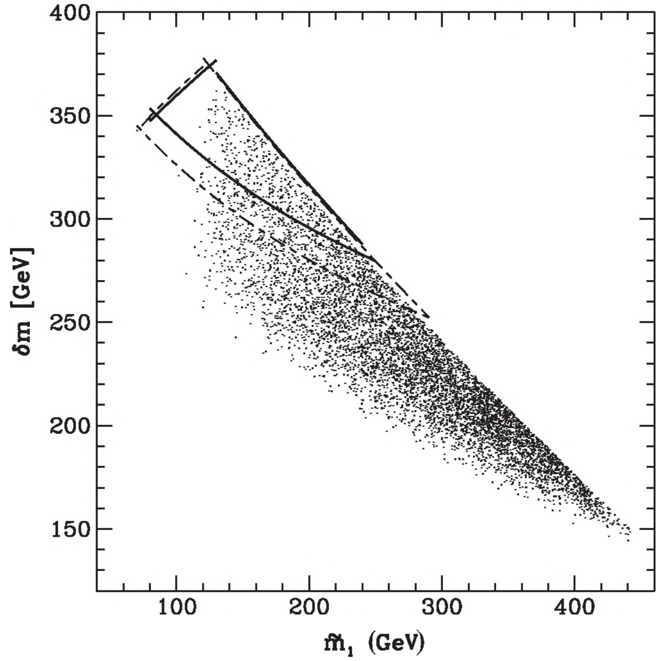

FIG. 1. The improved golden region: We have scanned the supersymmetric parameter space with constraints imposed from the bound on the Higgs mass, fine-tuning, and other experimental constraints including $b \to s\gamma$ to find an improved golden region; here we have fixed $\theta_t = \frac{\pi}{4}$ and $\tan\beta = 10$ in our "default scan" in parameter space. The fine-tuning parameter is set to be 33.3. For comparison, the area enclosed by the solid line shows the corresponding golden region previously found in Fig. 2 of [2] with the top-quark mass 171.4 GeV. The area enclosed by the dashed-dotted line corresponds to our value of the top-quark mass, 174.3 GeV. Note that our lowest value of $\delta m = 150$ GeV is lower than that in the previous work, as discussed in the text. (We have actually redrawn Perelstein and Spethmann's golden region using their code, fixing the D-terms in the $m_{\tilde{b}}$ mass [10].)

$$2.71 \times 10^{-4} < \mathrm{Br}(b \to s\gamma) < 4.39 \times 10^{-4}. \tag{6}$$

Whereas [2] noted that including this constraint was mostly beyond the scope of their paper, we have implemented this constraint throughout. Hence our results in Fig. 1 illustrate the "improved" golden region in the presence of this additional constraint (and of a more accurate calculation of the Higgs boson masses).

We note that [2] defined a benchmark point in their Table 1, with particular choices of the other parameters, and *did* include the $b \to s\gamma$ ratio when they checked this point using SUSPECT. SUSPECT gave them an acceptable $b \to s\gamma$ ratio for their benchmark model, but DARKSUSY (which includes better expressions for the branching ratio with next-to-leading-order corrections) gives an unacceptable value.

The golden region in Fig. 1 contains 7000 points satisfying all relevant bounds. The region is a triangle, with the lower boundary due to the constraint on the Higgs mass, the leftmost boundary due to the bounds on the ρ parameter, and the upper boundary due to fine-tuning. We now discuss each of these bounds in turn.

A. Lower boundary of golden triangle: Higgs mass

The lower boundary of the golden region triangle is set by bounds on the Higgs mass. The LEP2 lower bound on the standard model Higgs mass is [6]

$$m(h^0) \gtrsim 114 \text{ GeV}. \quad (7)$$

For generic MSSM parameter choices, the limit on the lightest Higgs is very close to this value as well, and we may use this bound. At tree level, the MSSM predicts $m(h^0) \le m_Z|\cos 2\beta|$, so that large loop corrections are required to satisfy this bound. The dominant one-loop corrections are from top and stop loops. The numerical package FEYNHIGGS [7] is incorporated into DARKSUSY to properly compute the Higgs mass and to apply the experimental bound. We note that the resulting boundary to the golden region that we find is slightly different from that of [2]: e.g. at $\tilde{m}_1 = 440$ GeV, our lowest value of $\delta m = 150$ GeV is quite a bit lower than the lowest value of $\delta m \sim 280$. The reason for this discrepancy is that their analytic approximations for the Higgs masses are less accurate than the values we find using the numerical package. (Our use of a different top-quark mass does not explain the discrepancy, as shown by the dashed-dotted line in Fig. 1.)

B. Upper boundary of golden triangle: Fine-tuning constraint

Fine-tuning of the Z mass also constrains the Higgs sector. At tree level, the Z mass in the MSSM is given by

$$m_Z^2 = -m_u^2\left(1 - \frac{1}{\cos 2\beta}\right) - m_d^2\left(1 + \frac{1}{\cos 2\beta}\right) - 2|\mu|^2, \quad (8)$$

where

$$\sin 2\beta = \frac{2b}{m_u^2 + m_d^2 + 2|\mu|^2}. \quad (9)$$

Since one of the two CP-even Higgs masses must satisfy $m_{u,d}^2 < 0$ for electroweak symmetry breaking, and since experimentally it is found that at least one of $m_{u,d}$, $|\mu| \gg m_Z$, cancellation of the terms on the right-hand side is required in order to get the right value of m_Z. Following Barbieri and Giudice [8], one may quantify this fine-tuning by computing

$$A(\xi) = \left|\frac{\partial \log m_Z^2}{\partial \log \xi}\right| \quad (10)$$

where $\xi = m_u^2, m_d^2, b, \mu$ are the relevant Lagrangian parameters. Then

$$A(\mu) = \frac{4\mu^2}{m_Z^2}\left(1 + \frac{m_A^2 + m_Z^2}{m_A^2}\tan^2 2\beta\right),$$
$$A(b) = \left(1 + \frac{m_A^2}{m_Z^2}\right)\tan^2 2\beta,$$
$$A(m_u^2) = \left|\frac{1}{2}\cos 2\beta + \frac{m_A^2}{m_Z^2}\cos^2\beta - \frac{\mu^2}{m_Z^2}\right| \times\left(1 - \frac{1}{\cos 2\beta} + \frac{m_A^2 + m_Z^2}{m_A^2}\tan^2 2\beta\right),$$
$$A(m_d^2) = \left|-\frac{1}{2}\cos 2\beta + \frac{m_A^2}{m_Z^2}\sin^2\beta - \frac{\mu^2}{m_Z^2}\right| \times\left|1 + \frac{1}{\cos 2\beta} + \frac{m_A^2 + m_Z^2}{m_A^2}\tan^2 2\beta\right|, \quad (11)$$

where it is assumed that $\tan\beta > 1$. The overall fine-tuning Δ is defined by adding the four A's in quadrature; values of Δ far above 1 indicate fine-tuning. Following [2], we require $\Delta \le 100$, corresponding to fine-tuning of 1% or better; this bound is implemented in our work and produces an upper bound of $\mu \lesssim 440$ GeV for $\tan\beta \gtrsim 0.5$. This matches the upper bound on μ found in [2]. We impose the constraints on the chargino mass from LEP2 chargino searches, which select $\mu \gtrsim 80$ GeV.

The upper boundary of the golden region triangle is determined by further restrictions on the fine-tuning. Quantum corrections to naturalness also constrain the size of the quantum corrections to the parameters in Eq. (8). Following [2], here we consider the largest correction in the MSSM, namely, the one-loop contribution to the m_u^2 parameter from top and stop loops:

$$\delta m_u^2 \approx \frac{3}{16\pi^2}\left(y_t^2(\tilde{m}_1^2 + \tilde{m}_2^2 - 2m_t^2) + \frac{(\tilde{m}_2^2 - \tilde{m}_1^2)^2}{4v^2}\sin^2 2\theta_t\right)\log\frac{2\Lambda^2}{\tilde{m}_1^2 + \tilde{m}_2^2}. \quad (12)$$

Here m_t is the top mass, Λ is the scale at which the logarithmic divergence is cut off, and finite (matching) corrections have been ignored. The correction to the Z mass induced by this effect is

$$\delta_t m_Z^2 \approx -\delta m_{H_u}^2\left(1 - \frac{1}{\cos 2\beta}\right). \quad (13)$$

To measure the fine-tuning between the bare (tree-level) and one-loop contributions, [2] introduced

$$\Delta_t = \left|\frac{\delta_t m_Z^2}{m_Z^2}\right|. \quad (14)$$

Choosing the maximum allowed value of Δ_t selects a region in the stop sector parameter space, $(\tilde{m}_1, \tilde{m}_2, \theta_t)$, whose shape is approximately independent of the other parameters. This constraint is outlined by the upper edge in Fig. 1, which corresponds to $\Delta_t \leq 33.3$ (3% fine-tuning). Note that the particular value of Δ_t depends on the scale Λ; we choose $\Lambda = 100$ TeV in this figure. As pointed out in [2], the shape of the Δ_t contours and the trend for the fine-tuning constraint to increase with the stop mass are independent of Λ.

C. Left boundary of golden triangle and other experimental constraints

The left boundary of the golden region triangle is set by measurements of the ρ parameter, which obtains corrections from stop and sbottom loops. We compute the ρ parameter using DARKSUSY and require

$$(2 - 8) \times 10^{-4} \leq \rho - 1 \leq (2 + 8) \times 10^{-4}, \qquad (15)$$

which represents the 2σ range from [9].

III. DARK MATTER

Now that we have found the improved golden region with the $b \to s\gamma$ bound implemented, we can investigate the properties of the dark matter in this region. Using DARKSUSY, we find the neutralino relic density for each set of MSSM parameter values in the improved golden region.

Figure 2 shows the relic density as a function of neutralino mass for all our default points in the golden region. As discussed previously, our default scan is defined by fixing $\tan\beta = 10$, $\theta_t = \pi/4$, and $\Delta_t = 33.3$ and scanning over other parameters. The lines illustrate the band that satisfies the cosmological requirement of $\Omega_\chi h^2$ in Eq. (1). Notice that there are points with the correct density for practically all neutralino masses in the golden region (with perhaps a tiny exception at the largest masses). Although most of the points in the figure have small $\Omega_\chi h^2$, we remind the reader that the density of points, in this and all the other plots, is arbitrary. The simulation uses a random number generator in the parameter domain. The dots are used for a plot as long as they satisfy the criteria for the golden region. Thus, the dot density does not necessarily have a physical meaning. It simply represents how the random number generator creates the dots.

In our default scan, we allowed the gaugino mass parameters $M_{1,2,3}$ to vary independently. If we instead impose the GUT relations

$$M_1 = \tfrac{5}{3}\tan^2\theta_W M_2, \qquad (16)$$

$$M_3 = \frac{\alpha_s(m_Z)}{\alpha}\sin^2\theta_W M_2, \qquad (17)$$

we still find points satisfying the cosmological constraint

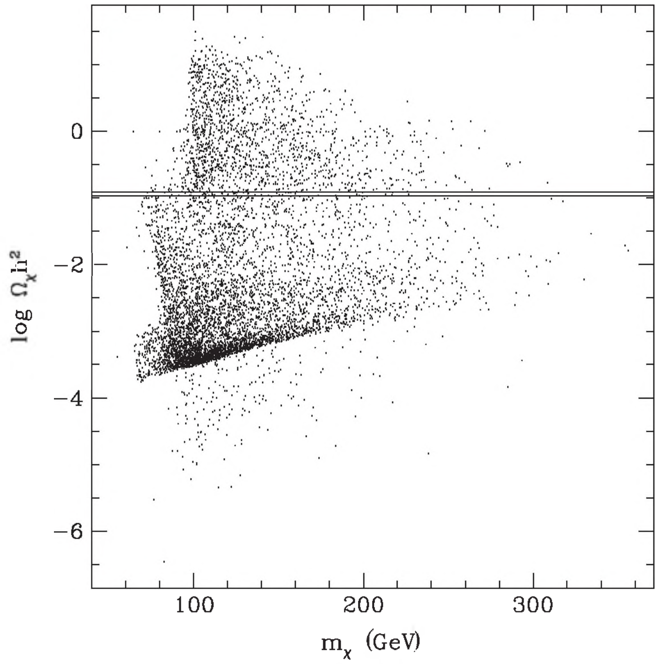

FIG. 2. Neutralino relic density $\Omega_\chi h^2$ as a function of neutralino mass m_χ for our default scan in parameter space ($\tan\beta = 10$, $\theta_t = \pi/4$, $\Delta_t = 33.3$). Each dot represents a point in supersymmetric parameter space that lies within the golden region. The horizontal band shows the 2σ range in the measured value of the cosmological density of cold dark matter [1]. Notice that there are points falling into the cosmological band for $m_\chi \leq$ 300 GeV.

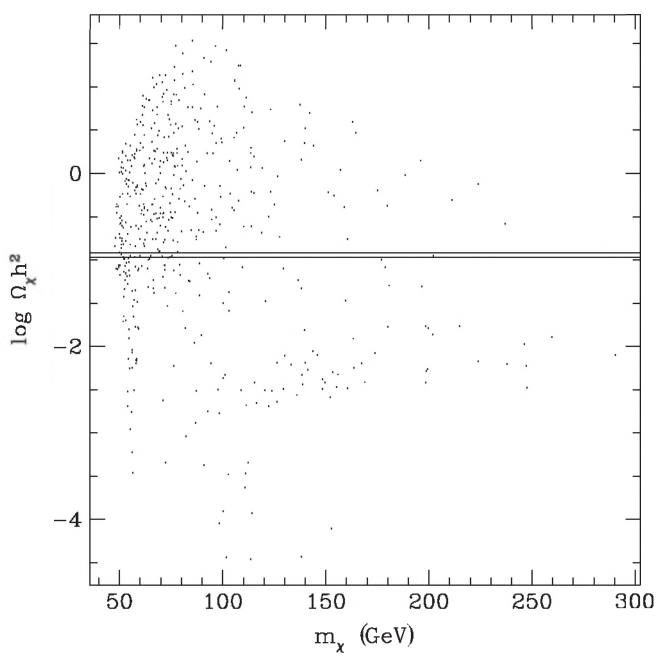

FIG. 3. Same as Fig. 2 except that M_1, M_2, and M_3 are related through the GUT relations, Eqs. (16) and (17). Notice that there are points falling into the cosmologically interesting band.

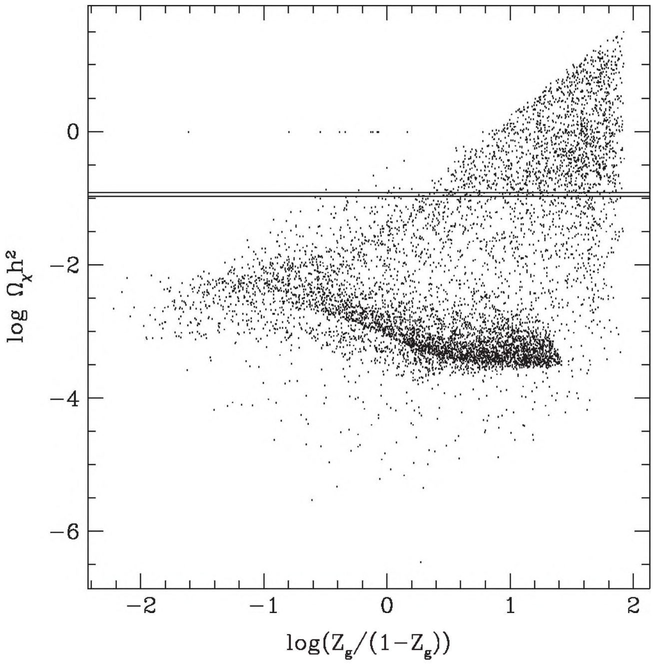

FIG. 4. Neutralino relic density $\Omega_\chi h^2$ as a function of $\frac{Z_g}{1-Z_g}$ for our default scan in parameter space. Each dot represents a point in supersymmetric parameter space that lies within the golden region. The horizontal band shows the 2σ range in the measured value of the density of cold dark matter [1]. Notice that there are points only above $\log\frac{Z_g}{1-Z_g} = 0$. One can see that the neutralino is typically predominantly gaugino rather than Higgsino.

on $\Omega_\chi h^2$. This is shown in Fig. 3, obtained by using the parameter ranges in Eqs. (2)–(5) but with the additional GUT conditions on M_1, M_2, and M_3 imposed.

To understand the properties of the points with the cosmologically interesting values of $\Omega_\chi h^2$, we have analyzed the dependence of $\Omega_\chi h^2$ in our default sample on all of the 11 independent parameters in the Lagrangian. Most of the parameters showed no interesting connection with $\Omega_\chi h^2$, except for M_1, and the gaugino fraction Z_g.

Figure 4 shows the relic density as a function of $Z_g/(1 - Z_g)$ where Z_g is the gaugino fraction of the neutralino. The denominator $1 - Z_g$ is the Higgsino fraction. Points in the cosmologically interesting band typically have $Z_g/(1 - Z_g) > 1$. Thus, the dark matter in the golden region that satisfies Eq. (1) is predominantly gaugino rather than Higgsino.

Figures 5(a) and 5(b) plot the relic density as a function of M_1, the mass of the $U(1)_Y$ gaugino. Figure 5(a) is for our default scan, while Fig. 5(b) is for an extended scan of 1700 points in which $\tan\beta$ varies in the range 0.5 to 30 and M_1 is allowed to be as large as 2000 GeV. One can see that points with the right relic density have $M_1 < 300$ GeV.

We find that some models, but not all, have coannihilations; we find chargino-neutralino, stau-neutralino, and stop-neutralino coannihilations.

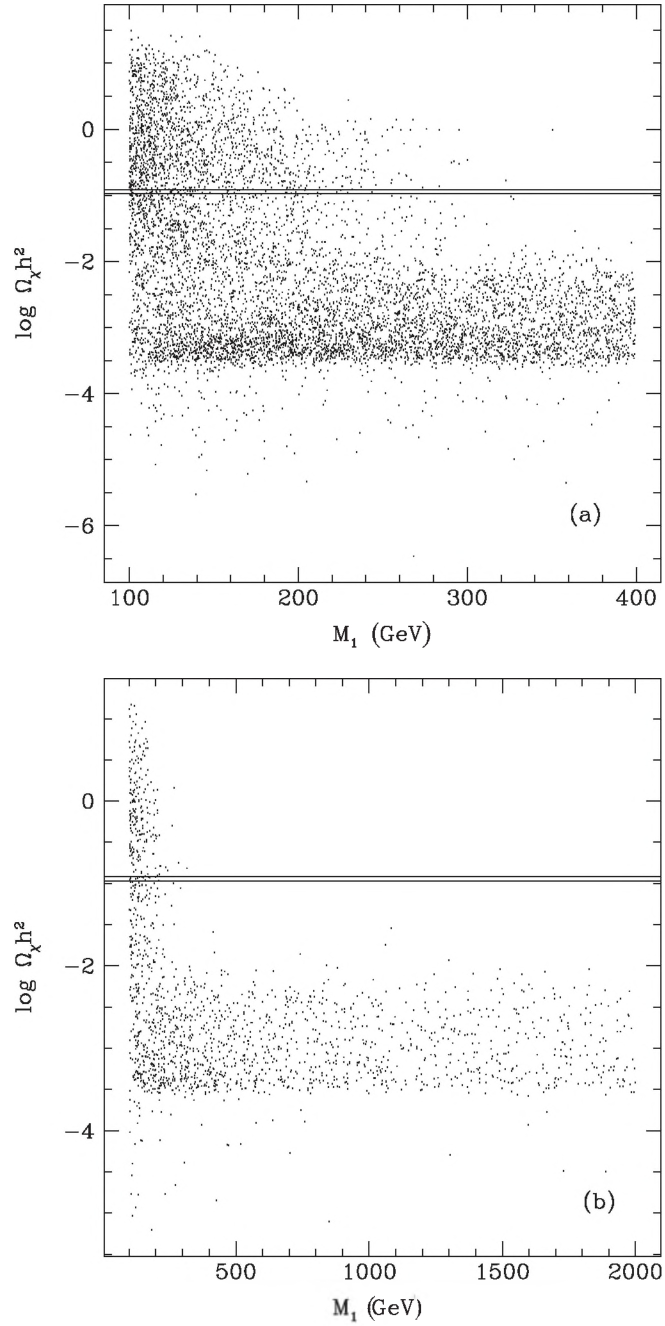

FIG. 5. Neutralino relic density $\Omega_\chi h^2$ as a function of M_1 for (a) our default scan in parameter space and (b) an extended scan with $0.5 < \tan\beta < 30$ and $100\text{ GeV} < M_1 < 2000$ GeV. Each dot represents a point in supersymmetric parameter space that lies within the golden region. The horizontal band shows the 2σ range in the measured value of the density of cold dark matter [1]. Notice that there are points in the golden region with the right cosmological neutralino density provided $M_1 < 300$ GeV.

IV. CONCLUSION

In conclusion, we have imposed further experimental bounds ($b \to s\gamma$) on the golden region found by [2] and have searched for subsets of this region which provide today's dark matter density in the form of neutralinos.

We found that $M_1 < 300$ GeV is required, and that when the neutralino is the dark matter in the golden region it is predominantly gaugino. In the future, we plan to examine direct and indirect detection rates in concert with LHC tests of the golden region.

ACKNOWLEDGMENTS

K. F. acknowledges support from the DOE and MCTP via the University of Michigan. P. G. and J. K. acknowledge NSF Grant No. PHY-0456825. K. F. thanks the Physics Department at the University of Utah for hospitality. J. K. acknowledges conversations with Ludmila Levkova on QCD. We thank Maxim Perelstein and Christian Spethmann for sharing their code with us and for helpful discussions. An allocation of computer time from the Center for High Performance Computing at the University of Utah is gratefully acknowledged.

[1] G. Hinshaw *et al.* arXiv:0803.0732 [Astrophys. J. (to be published)].
[2] M. Perelstein and C. Spethmann, J. High Energy Phys. 04 (2007) 070.
[3] R. Kitano and Y. Nomura, Phys. Rev. D **73**, 095004 (2006).
[4] P. Gondolo, J. Edsjo, P. Ullio, L. Bergstrom, M. Schelke, and E. A. Baltz, J. Cosmol. Astropart. Phys. 07 (2004) 008.
[5] S. Chen *et al.* (CLEO Collaboration), Phys. Rev. Lett. **87**, 251807 (2001); B. Aubert *et al.* (*BABAR* Collaboration), arXiv:hep-ex/0507001; P. Koppenburg *et al.* (Belle Collaboration), Phys. Rev. Lett. **93**, 061803 (2004); E. Barberio *et al.* [Heavy Flavor Averaging Group (HFAG)], arXiv:hep-ex/0603003.
[6] S. Schael *et al.* (ALEPH Collaboration), Eur. Phys. J. C **47**, 547 (2006).
[7] The FEYNHIGGS package can be downloaded from http://wwwth.mppmu.mpg.de/members/heinemey/feynhiggs/index.html.
[8] R. Barbieri and G. F. Giudice, Nucl. Phys. **B306**, 63 (1988).
[9] W. M. Yao *et al.* (Particle Data Group), J. Phys. G **33**, 1 (2006).
[10] M. Perelstein (private communication).